Medicinal Plant Biology

ARTICLE

Open Access

https://doi.org/10.48130/mpb-0026-0018

Medicinal Plant Biology **2026**, 5: e023

Comparative metabolomic and transcriptomic analyses of metabolic differentiation between two *Spiranthes* species and cultivation effects on *Spiranthes sinensis*

Feng-pan Wang[1*], Pan-pan Zhao[2*], Li-jun Chen[1], Shao-rong Zhou[1] and Yue-hong Yan[3]

[1] *Key Laboratory of National Forestry and Grassland Administration on Dendrobium officinale, The Orchid Conservation and Research Center of Shenzhen, Shenzhen 518114, China*

[2] *Guangzhou Academy of Agriculture and Rural Sciences, Guangzhou 510308, China*

[3] *Shanghai Chenshan Botanical Garden (Chenshan Scientific Research Center of CAS Center for Excellence in Molecular Plant Sciences), Shanghai 201602, China*

* Correspondence: duibian@126.com (Wang FP); zpp19891004@163.com (Zhao PP)

Abstract

Spiranthes sinensis (Pers.) Ames, the officially recognized botanical source of the traditional Chinese medicinal herb '*Pan long sen*', is widely documented in the *Chinese Materia Medica*. In ethnobotanical practice, however, this species is frequently substituted with other geographically widespread congeners, particularly *S. australis*, despite a paucity of comparative data on their phytochemical profiles. While preliminary pharmacological studies have identified bioactive phenanthrenes, flavonoids, and coumarins in *S. sinensis*, a comprehensive understanding of the full-spectrum metabolomes of *Spiranthes* species and how cultivation influences their chemical profiles is still lacking. We performed comparative metabolomics and transcriptomics to compare wild *S. sinensis* and *S. australis*, and to assess how cultivation and growth duration affect *S. sinensis*. A total of 2,593 metabolites were detected across four groups, including 1,479 secondary metabolites; flavonoids were the dominant class. *S. australis* accumulated a greater diversity and abundance of metabolites than *S. sinensis*, with KEGG enrichment analysis revealing heightened activity in phenylpropanoid biosynthesis. Cultivated *S. sinensis* exhibited broader metabolite enrichment than wild plants, particularly in amino acid derivatives, flavonoids, terpenoids, alkaloids, and lipids. Transcriptomic analysis showed that cultivation induced large-scale differential gene expression, with up-regulated genes significantly enriched in secondary metabolite and flavonoid biosynthesis pathways, supporting the enhanced metabolic capacity under managed conditions. Strikingly, a developmental shift occurred between one- and two-year-old cultivated plants: younger individuals accumulated primary and non-flavonoid secondary metabolites broadly, whereas older plants specifically upregulated flavonoid biosynthesis, with 35 flavonoid-related genes highly expressed in two-year-old plants versus only nine in one-year-old plants, consistent with the metabolomic enrichment of flavonoids. These findings not only elucidate the chemotaxonomic relationship between *S. sinensis* and *S. australis* but also establish extended cultivation duration as a critical agronomic strategy for maximizing flavonoid yield in *S. sinensis*.

Keywords: *Spiranthes sinensis*, *Spiranthes australis*, Comparative metabolomics, Artificial cultivation

Citation: Wang FP, Zhao PP, Chen LJ, Zhou SR, Yan YH. 2026. Comparative metabolomic and transcriptomic analyses of metabolic differentiation between two *Spiranthes* species and cultivation effects on *Spiranthes sinensis*. *Medicinal Plant Biology* 5: e023 https://doi.org/10.48130/mpb-0026-0018

Introduction

'Pan long sen' was first recorded in *Diannan Bencao*, a distinguished regional herbal compendium compiled during the Ming Dynasty (1436 CE), for its traditional therapeutic functions of replenishing *qi*, nourishing *yin*, clearing heat, and detoxification. Since then, it has been widely utilized both as a folk medicinal herb and as a nutritive edible plant in traditional Chinese communities. According to the *Chinese Materia Medica* (State Administration of Traditional Chinese Medicine), the official botanical source of '*Pan long sen*' is *Spiranthes sinensis* (Pers.) Ames; the dried whole plant or fleshy tuberous roots are used as the crude drug, and it is traditionally prescribed for post-illness debility, chronic cough, neurasthenia, sore throat, diabetes mellitus, and nephritis. The pharmacological activities of Chinese medicinal herbs are primarily attributed to their diverse array of secondary metabolites, such as flavonoids, terpenoids, alkaloids, and phenolic acids[1,2]. Consequently, the identification and experimental validation of bioactive constituents from '*Pan long sen*' remain a central focus of contemporary pharmacological research on this traditional Chinese medicinal herb[3–5].

Over the past two decades, phytochemical studies have consistently demonstrated that *Spiranthes* species, particularly *S. sinensis* (Pers.) Ames, are rich sources of structurally diverse and biologically active secondary metabolites[4–6]. A chemotaxonomic hallmark of the genus *Spiranthes* is its prolific biosynthesis of phenanthrene derivatives, notably 9,10-dihydrophenanthrenes[7]. Specific compounds, including sinensols A–F[3], spiranthols A–C[8,9], and various prenylated dihydrophenanthrenes, have been repeatedly isolated from *S. sinensis* and exhibit a broad spectrum of pharmacological activities, such as anti-inflammatory[10], antitumor[11], and anti-adipogenic effects[12]. In addition, *S. sinensis* is recognized as a rich source of diverse flavonoids, another major class of bioactive secondary metabolites with well-documented health-promoting properties[4,5]. Beyond phenanthrenes and flavonoids, *S. sinensis* also accumulates substantial quantities of other bioactive constituents, including phenolic acids[4,13], coumarins[14], and phytosterols[4]. Collectively, these metabolites underlie the documented bioactivities of *S. sinensis*, including acetylcholinesterase inhibition, suggesting therapeutic potential in Alzheimer's disease[15], and the enhancement of cellular viability under metabolic stress[10]. Together, these findings underscore that the medicinal properties of *Spiranthes* are intrinsically linked to its complex and species-specific metabolomic profile.

Although the *Chinese Materia Medica* officially recognizes *S. sinensis* as the sole botanical source of '*Pan long sen*', folk practitioners

https://doi.org/10.48130/mpb-0026-0018

commonly substitute it with other widely distributed congeners as pragmatic alternatives, particularly *S. australis* (R.Br.) Lindl. To date, all commercially available '*Pan long sen*' is sourced exclusively from wild-harvested *S. sinensis*, with no documented cases of successful artificial cultivation. This dual dependence on wild harvesting and the prevailing taxonomic ambiguity in ethnobotanical practice raises a critical question: to what extent do the metabolite profiles, fundamental to their medicinal efficacy, differ between *Spiranthes* species, and how are they modulated by artificial cultivation? While numerous studies have elucidated the chemical constituents of wild *S. sinensis*[3–7], comprehensive comparative metabolomic data between *S. sinensis* and its congener *S. australis* remain scarce. To date, the impact of cultivation practices on the global metabolomic profile of *Spiranthes* remains unexplored. It is well documented in phytochemical research that environmental conditions, agronomic interventions, and domestication processes can substantially influence the biosynthesis and accumulation of secondary metabolites in medicinal plants[16]. Recent studies have shown that *in vitro*-cultivated *Hypericum bilgehan-bilgilii* exhibits enhanced physiological traits and elevated antioxidant capacity[17], while cultivated *Lonicera japonica* has been found to accumulate significantly higher levels of chlorogenic acid compared to its wild counterparts[18]. Consequently, a comprehensive comparative analysis is imperative, not only to ensure the quality and authenticity of future cultivated materials but also to clarify chemotaxonomic relationships between these two closely related congeners.

Although '*Pan long sen*' is not currently included in the *Chinese Pharmacopoeia*, it has been extensively documented in regional and ethnobotanical herbal texts across China. Historically, traditional practitioners developed numerous effective formulations based on its perceived therapeutic properties, which played a crucial role in managing common ailments and supporting community health in eras when access to modern medicine was limited. In this study, we performed metabolomic and transcriptomic analyses to systematically characterize interspecific metabolic divergence between *S. sinensis* and *S. australis*, as well as the impact of artificial cultivation and growth duration on the metabolite profiles of *S. sinensis*. To address these objectives, we analyzed four sample groups: wild *S. sinensis*, wild *S. australis*, and one- and two-year-old cultivated *S. sinensis*. Widely targeted metabolomics was employed for comprehensive metabolite profiling, complemented by transcriptome sequencing to elucidate the underlying transcriptional regulatory mechanisms[19]. Specifically, we sought to answer two key questions: (1) which metabolic features underlie the chemotaxonomic distinction between the two *Spiranthes* species, and (2) how artificial cultivation and extended growth duration reprogram the metabolomic and transcriptomic landscapes of *S. sinensis*. Our findings provide comprehensive insights into the metabolic difference between these two species and cultivation-induced metabolic reprogramming in *S. sinensis*, thereby offering a scientific foundation for the sustainable utilization and quality optimization of this valuable medicinal orchid.

Materials and methods

Plant materials

The collection of wild *Spiranthes* specimens was conducted in accordance with the Wild Plant Protection Regulation of the People's Republic of China. None of the sampled wild species is listed in the National Key Protected Wild Plant List (2021 revision). Wild individuals of *S. sinensis* and *S. australis* were collected from Guangzhou (Guangdong Province) and Chenzhou (Hunan Province), respectively. Sampling sites were deliberately selected to avoid any legally protected nature reserves. Both collection sites are situated in subtropical regions dominated by mixed evergreen–deciduous broad-leaved forests. At each location, 10–15 plants were carefully uprooted, ensuring the complete retention of root systems and aerial parts. Species identification was performed through detailed morphological dissection and comparison with the original descriptions of the holotype specimens and relevant taxonomic literature (Flora of China, Vol. 25, 2009)[20]. The key diagnostic characters used for identification included: for *S. sinensis*—inflorescence axis, ovary, and bracts glabrous, pink flowers, stigma subdiscoid, with rostellum; for *S. australis*—inflorescence axis, ovary, and bracts glandular pubescent, pink flowers, stigma bilobed, with rostellum. Voucher specimens have been temporarily deposited at the Herbarium of the Orchid Conservation and Research Center of Shenzhen (Shenzhen, Guangdong, China) under accession numbers YYH20968 (*S. sinensis*) and YYH20980 (*S. australis*). To mitigate potential metabolic perturbations arising from site-specific environmental conditions or post-harvest stress, all collected specimens were immediately transplanted into square terracotta pots (20 cm × 20 cm) filled with a well-drained substrate composed of bark, gravel, and humus, in a volumetric ratio of 4:1:1, and subsequently acclimatized under controlled greenhouse conditions. One month after acclimatization, whole plants were harvested. Roots and leaves were thoroughly rinsed with tap water to remove adhering soil, followed by gentle scrubbing of root surfaces with a soft brush. Samples were then rinsed 2–3 times with ultrapure water, blotted dry with absorbent paper, cut into 0.5 cm segments, homogenized, immediately flash-frozen in liquid nitrogen, and stored at −80 °C until analysis. Three biological replicates were prepared for each sample type.

Mature capsules were harvested from wild *S. sinensis*. Following surface cleaning and air-drying, the capsules were stored in paper envelopes under cool, dark, and dry conditions until natural dehiscence. Seeds were aseptically extracted using fine-tipped forceps and transferred into 15 mL centrifuge tubes, filled to no more than one-third of their capacity. Surface sterilization was carried out by immersing the seeds in 10 mL of 2% (v/v) sodium hypochlorite solution supplemented with 0.02% (v/v) Triton X-100, followed by agitation on an orbital shaker for 10 min. After brief centrifugation to pellet the seeds, the disinfectant was discarded, and the seeds were rinsed three times with sterile distilled water. Sterilized seeds were then deposited onto sterile filter paper and held until sowing. For germination, seeds were evenly distributed on half-strength Murashige and Skoog (1/2 MS) basal medium supplemented with 1.0 mg·L^{-1} naphthaleneacetic acid (NAA), 1.6 mg·L^{-1} 6-benzylaminopurine (6-BA), and 2.0 g·L^{-1} activated charcoal. Using flame-sterilized forceps, individual seeds were gently pressed onto the surface of the solidified medium to ensure contact without embedding. Cultures were incubated in a growth chamber maintained at 25 ± 1 °C under a 16 h photoperiod (light intensity: 1,500–3,000 lux) and 60%–70% relative humidity.

Once protocorm-derived plantlets attained a height of 2–3 cm, they were subcultured onto a rooting medium containing 1.5 mg·L^{-1} indole-3-butyric acid (IBA) to stimulate root formation. When plantlets reached 4–5 cm in height with well-developed root systems, they were carefully removed from the culture vessels, and residual agar was gently rinsed off with sterile water. The entire seedlings were then immersed in a 0.1% (w/v) broad-spectrum

fungicide solution for 5–10 min as a prophylactic measure. Subsequently, the treated plantlets were transplanted into plastic pots filled with a well-draining substrate composed of bark, humus, and gravel in a volumetric ratio of 4:1:1, thoroughly irrigated, and transferred to a greenhouse for acclimatization. To maintain high humidity during the initial hardening phase, pots were covered with transparent plastic film for 7–10 d, after which the cover was gradually removed over several days to avoid desiccation stress. Thereafter, plants were maintained under standard cultivation practices. Sampling of these cultivated plants followed the identical protocol employed for wild-collected individuals.

Broadly targeted metabolomics assay

Metabolomic profiling was performed by Metware Biotechnology Co., Ltd. (Wuhan, China). Approximately 5 g of pre-weighed, flash-frozen plant material was lyophilized to constant weight using a freeze dryer (Scientz-100F, Ningbo Scientz Biotechnology Co., China), ground into a homogeneous powder with a ball mill, and passed through a 60-mesh sieve. An aliquot of 50 mg of the resulting powder was accurately weighed into a 2 mL centrifuge tube, followed by the addition of 1,200 μL of ice-cold 70% (v/v) methanol extraction solvent containing 10 mg·L^{-1} 2-chlorophenylalanine as an internal standard (Aladdin, Shanghai, China). The mixture was extracted via ultrasonication at 4 °C for 3 h, with brief vortexing (30 s) every 30 min (six cycles total). After extraction, samples were centrifuged at 12,000 × *g* for 3 min at 4 °C. The supernatant was filtered through a 0.22 μm nylon syringe filter (Merck Millipore, Darmstadt, Germany) and transferred into glass autosampler vials for analysis.

Chromatographic separation was carried out on an ultra-performance liquid chromatography system (ExionLC™ AD, Sciex, Framingham, MA, USA) coupled online to a QTRAP® 6500+ triple quadrupole-linear ion trap mass spectrometer (Applied Biosystems, Foster City, CA, USA). Analytes were resolved on a Waters ACQUITY UPLC HSS T3 C18 column (1.8 μm, 100 mm × 2.1 mm i.d.; Waters Corporation, Milford, MA, USA) maintained at 40 °C. The mobile phase consisted of solvent A (ultrapure water with 0.01% acetic acid and 5 mmol·L^{-1} ammonium acetate) and solvent B (acetonitrile with 0.01% acetic acid). A gradient elution program was applied at a flow rate of 0.35 mL·min^{-1} with the following profile: 0 min, 95% A; 1 min, 60% A; 7 min, 50% A; 12 min, 25% A; 14 min, 5% A; 16 min, 95% A. The injection volume was 3 μL.

Mass spectrometry was operated in electrospray ionization (ESI) mode with simultaneous data acquisition in both positive and negative ion polarities. Detection was performed in multiple reaction monitoring (MRM) mode. Source parameters were optimized as follows: ion source temperature, 550 °C; nebulizer gas (GS1) and heater gas (GS2) pressure, 55 psi each; ion spray voltage, +5,500 V (positive mode) and –4,500 V (negative mode); collision gas (high-purity nitrogen) set to medium intensity. For each metabolite, one to three specific precursor-to-product ion transitions (Q1/Q3) were monitored, with declustering potential (DP) and collision energy (CE) individually optimized based on authentic chemical standards or published literature.

Metabolites were identified by comparing their retention times, precursor-to-product ion transitions, and fragmentation patterns against the Metware Database (MWDB v3.0), which contains over 5,000 authentic standards. For metabolites without commercially available standards, identification was based on high-confidence matching of MS/MS spectra to those reported in the literature or public databases (MassBank, HMDB, and MoNA). Quantification was performed using the MRM mode with the internal standard (2-chlorophenylalanine) for normalization. A total of 1 mg·L^{-1} of 2-chloro-L-phenylalanine was spiked into the system as a quality control to monitor instrument response stability. Peak integration and manual inspection were carried out using MultiQuant 3.0 software (Sciex, Framingham, MA, USA). A pooled quality control (QC) sample was prepared by mixing equal aliquots of all individual samples and was injected every ten analytical runs to monitor instrument stability and reproducibility. Metabolites with a relative standard deviation (RSD) > 30% in QC samples were excluded from downstream analysis. The coefficient of variation (CV) of the internal standard across all injections was maintained below 15%.

Transcriptome sequencing, analysis, and validation

Total RNA was isolated from flash-frozen plant tissues using the RNeasy Plus Mini Kit (Qiagen, Germany). RNA quality was evaluated based on ribosomal RNA integrity (28S/18S band sharpness) via capillary electrophoresis on a Qsep400 system (Bioptic, China), while RNA concentration was quantified with a Qubit 4.0 Fluorometer (Thermo Fisher Scientific, USA). Only samples exhibiting an RNA Integrity Number (RIN) exceeding 7.0 were selected for library preparation. Stranded cDNA libraries were constructed following a standard Illumina-compatible workflow: polyadenylated mRNA was enriched using oligo(dT)-conjugated magnetic beads, chemically fragmented, and reverse-transcribed into first- and second-strand cDNA. After end repair, adapter ligation, and size selection, libraries were amplified by PCR. Final library quality and concentration were confirmed using fluorometric quantification (Qubit), fragment analysis, and qPCR, with all libraries meeting the minimum requirement of > 2 nM for sequencing.

Paired-end sequencing was carried out on an Illumina NovaSeq 6000 platform (Illumina Inc., USA). Raw reads were subjected to quality control using fastp (v0.23.2) under default settings to trim adapter sequences, remove reads containing excessive N bases, and discard low-quality reads, yielding high-confidence clean reads for downstream analysis. Due to the absence of a high-quality reference genome for *Spiranthes* species, a *de novo* transcriptome assembly was performed using Trinity (v2.15.1). Transcript abundance was estimated in transcripts per million (TPM) and raw read counts were generated using Salmon (v1.9.0) in alignment-free mode, with bias correction enabled. These estimated counts were then imported into R for differential expression analysis using the DESeq2 package (v1.36.0). Genes were considered significantly differentially expressed if they exhibited an absolute $\log_2$ fold change ≥ 1 and a false discovery rate (FDR)-adjusted *p*-value < 0.05.

The sequencing generated 38.0–75.8 million raw reads for the 12 individual samples. After quality filtering, 37.1–73.5 million clean reads were retained, with Q30 values ranging from 96.6% to 97.3%, indicating high sequencing quality (Supplementary Table S1). Functional annotation of assembled unigenes was performed by aligning predicted protein sequences against multiple public databases, namely NR (non-redundant), Swiss-Prot, and TrEMBL, using DIAMOND (v2.1.6) in blastx mode (e-value cutoff: 1e^{-5}). Additionally, conserved protein domains were identified by searching unigene-derived amino acid sequences against the Pfam database with HMMER (v3.3.2). To elucidate biological roles, Gene Ontology (GO) and Kyoto Encyclopedia of Genes and Genomes (KEGG) enrichment analyses were carried out on the differentially expressed gene sets using the clusterProfiler package (v4.4.4) in R (Yu et al.)[21]. GO annotations were retrieved from the Gene Ontology knowledgebase

https://doi.org/10.48130/mpb-0026-0018

(http://geneontology.org)[22]. KEGG pathway annotations were retrieved from the KEGG database (www.kegg.jp)[23]. Enriched terms and pathways were considered statistically significant at an FDR-adjusted p-value < 0.05.

We performed qRT-PCR assays to validate the expression of several well-annotated unigenes identified in the transcriptomic analysis. Total RNA extraction, cDNA synthesis, and qRT-PCR assays were carried out following the methods described in a previous study[24]. The *actin* gene was used as the internal control. Unigene-specific primer pairs were synthesized by Sangon Biotech Co., Ltd. (Shanghai, China), and their sequences are listed in Supplementary Table S2. The qRT-PCR validation revealed that, except for a few individual unigenes, the expression patterns of the majority of tested unigenes in the four samples matched those observed in the transcriptomic FPKM profiles (Supplementary Fig. S1).

Statistical analysis

Unsupervised principal component analysis (PCA) was performed using the prcomp function in R (v4.3.1). Orthogonal partial least squares discriminant analysis (OPLS-DA) was conducted using the ropls package (v1.32.0) to maximize class separation. Model quality was assessed by R^2Y and Q^2 values, with model validation performed using 200 permutation tests. Differential metabolite selection: Variable importance in projection (VIP) values were calculated from OPLS-DA models. Metabolites with VIP > 1, absolute fold change (FC) > 2, and Student's t-test p-value < 0.05 were considered significantly differentially enriched. To control for false positives, p-values were adjusted using the Benjamini–Hochberg false discovery rate (FDR) method; metabolites with FDR-adjusted p-value < 0.05 were retained as statistically significant. K-means clustering: Unsupervised clustering of metabolite abundance profiles was performed using the K-means function in R (v4.3.1). The optimal number of clusters (k = 6) was determined by the elbow method based on within-cluster sum of squares. KEGG enrichment analysis: Pathway enrichment of differentially accumulated metabolites was performed using the KEGG Mapper tool and the clusterProfiler package (v4.4.4) in R. Enriched pathways were considered significant when the FDR-adjusted p-value < 0.05. Differential abundance scores were calculated based on $\log_2$FC of metabolites within each pathway to indicate overall direction of pathway-level changes.

Results

Metabolomic analysis of *Spiranthes* plants

According to the *Chinese Materia Medica*, *Spiranthes* plants are used as fleshy roots or whole herbs for medicinal purposes. Therefore, we selected healthy entire plants for this study (Fig. 1a–d) and employed widely targeted metabolomics to determine the full-spectrum metabolite content in all samples. Unsupervised PCA was performed on the metabolomic data. The PCA score plot (Fig. 1e) showed that the first principal component (PC1) and second principal component (PC2) explained 41.17% and 29.63% of the variance, respectively, with a cumulative value of 70.80%, indicating that the model could adequately explain the metabolite differences among the four plant materials. The distribution pattern in the score plot revealed a clear separation between *S. sinensis* and *S. australis* samples; wild and cultivated *S. sinensis* also separated from each other and clustered independently within their respective 95% confidence intervals. These results suggest significant differences in the metabolomic profiles among the samples, reflecting distinct metabolic signatures between *S. sinensis* and *S. australis*. Furthermore, the separation between the two cultivated *S. sinensis* samples of different growth years was smaller than that between cultivated and wild *S. sinensis*, indicating that the effect of growth year on metabolite composition under the same habitat was less pronounced than that of habitat variation.

A total of 2,593 metabolites were detected across the four *Spiranthes* samples, among which 1,479 were secondary metabolites, showing a higher abundance than primary metabolites. The total number of detected metabolites varied among the four samples, with the two-year-old artificially cultivated *S. sinensis* possessing the highest metabolite count (Supplementary Fig. S2). The most abundant metabolite classes in *Spiranthes* were flavonoids (428), amino acids and their derivatives (358), alkaloids (304), lipids (266), terpenoids (221), phenolic acids (211), organic acids (113), and nucleotides and their derivatives (97) (Fig. 1f). Flavonoids and phenanthrenes are key bioactive constituents in Orchidaceae[11,25]. Metabolomic profiling revealed that flavonoids were the most abundant chemical class in the two *Spiranthes* species, encompassing all seven common subclasses found in seed plants, namely flavones, isoflavones, flavonols, flavanols, anthocyanins, dihydroflavones, and dihydroflavonols (Fig. 1g), with flavones and flavonols being the most predominant. In addition, six aurone compounds were also identified. Table 1 presents the top 20 flavonoid metabolites with the highest relative contents in *S. sinensis* and *S. australis*, most of which were glycoside derivatives of flavonoids. A total of 81 quinones were detected across the four materials, including 60 phenanthraquinones (Fig. 1f). Phenanthraquinones are quinone derivatives of phenanthrenes, which are characteristic compounds of orchids such as *Spiranthes*[26]. Furthermore, 39 stilbenes and their derivatives were identified in *Spiranthes* (Fig. 1f), compounds that share similar biosynthetic pathways and biological activities with flavonoids. From the perspective of biological functions, *Spiranthes* plants are rich in both naturally occurring bioactive compounds (Supplementary Table S3), such as quercetin, protocatechuic acid, epicatechin, catechin, and dendrobine, as well as various nutritional metabolites, including amino acids, nucleotides, vitamins, organic acids, sugars, and free fatty acids.

Comparison of full-spectrum metabolites between *S. sinensis* and *S. australis*

S. sinensis and *S. australis* are the most widely distributed *Spiranthes* species in China, with large wild resources and relatively easy accessibility, and they are commonly used as herbal medicines by local people. We compared the full-spectrum metabolomes of these two species using metabolomics. A total of 2,267 and 2,286 metabolites were detected in *S. sinensis* and *S. australis*, respectively (Supplementary Fig. S2), of which 2,098 were common to both species, while 169 and 188 were specific to each species, respectively (Supplementary Fig. S3). In terms of metabolite classes, the most differential metabolites between the two species were flavonoids, lipids, and terpenoids (Supplementary Fig. S4). Based on different metabolite categories, we analyzed sample correlations (Supplementary Fig. S5). The correlation coefficient was lowest when comparing flavonoid relative contents, ranging from 0.79 to 0.81 (Supplementary Fig. S5d); when comparing primary metabolite relative contents, the correlation coefficients were higher, ranging from 0.94 to 0.95 (Supplementary Fig. S5b). This indicates that flavonoids are likely the most distinct metabolites between *S. sinensis* and *S. australis*, whereas primary metabolites show less difference

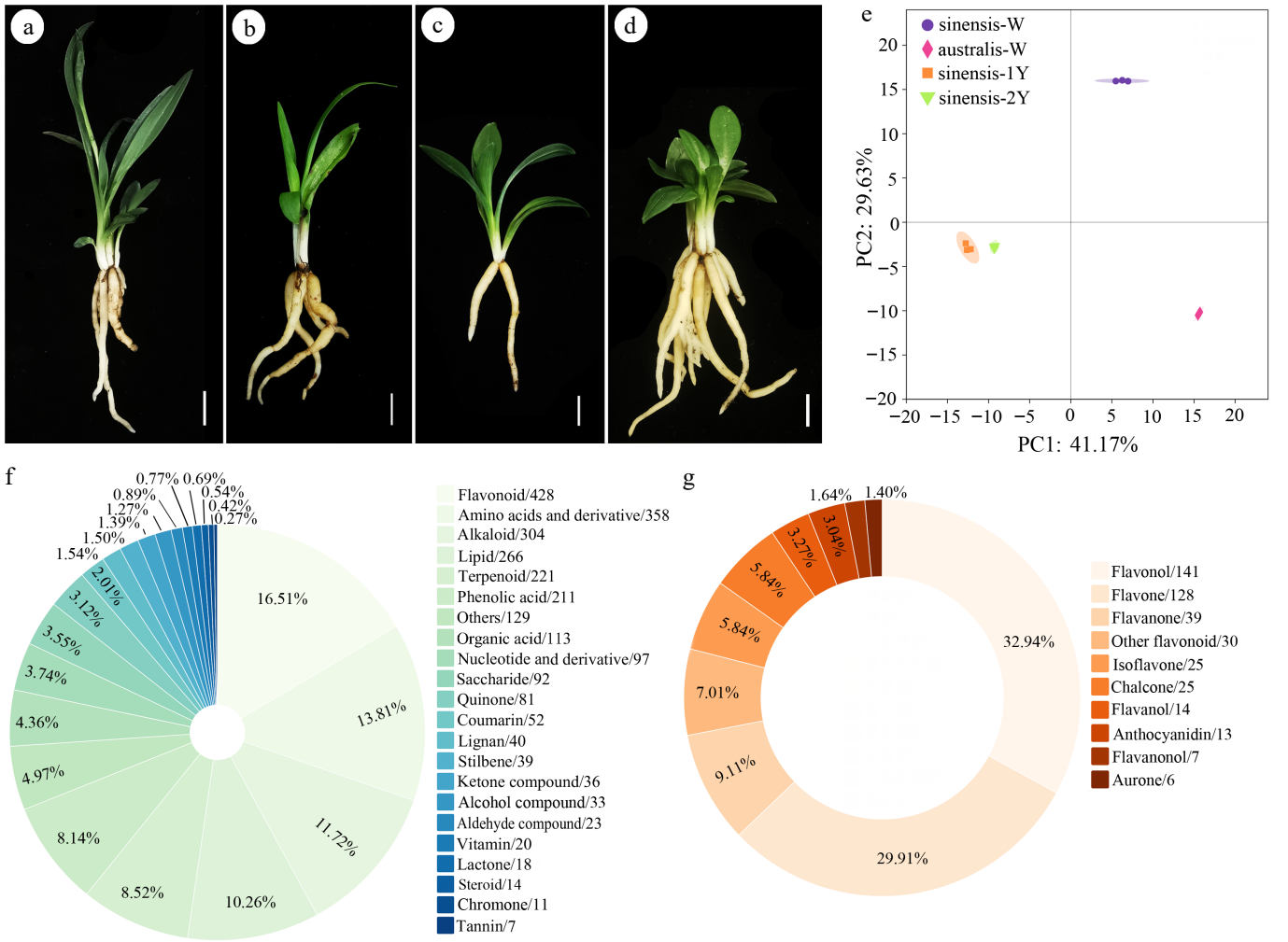

Fig. 1 *Spiranthes* plants and their metabolite composition. (a) *S. sinensis*-wild. (b) *S. australis*-wild. (c) One-year-old *S. sinensis* cultivated from seed. (d) Two-year-old *S. sinensis* cultivated from seed. (e) Principal component analysis of the comprehensive metabolomic profiles from the four *Spiranthes* samples. (f) Different classifications of metabolites in the *Spiranthes* plants. (g) Different types of flavonoid compounds in the *Spiranthes* plants. White scale bar = 2 cm.

between the two species. Based on the relative content of each metabolite, Fig. 2b shows the abundance distribution in both species, preliminarily suggesting that *S. australis* accumulates more metabolites than *S. sinensis*. Further K-means clustering analysis of all metabolites revealed that 347 and 649 metabolites were relatively more abundant in *S. sinensis* and *S. australis*, respectively (Supplementary Figs. S6 and S7), confirming that wild *S. australis* accumulates more metabolites than *S. sinensis*.

Using a VIP (variable importance in projection) value > 1 as the threshold, we screened for metabolites significantly enriched in *S. australis* compared to *S. sinensis*, with criteria of fold change > 2 and *p*-value < 0.05. The volcano plot (Fig. 2a) showed that 526 metabolites were significantly enriched in wild *S. australis* relative to *S. sinensis*; these metabolites were mainly flavonoids (97), amino acid derivatives (82), alkaloids (62), quinones (38), phenolic acids (35), lipids (35), stilbenoids (26), and terpenoids (24) (Fig. 2c; Supplementary Table S4). Based on the KEGG pathways of these differentially enriched metabolites, Fig. 2d displays the top 20 most significantly enriched pathways. The top five pathways, biosynthesis of stilbenoids II, biosynthesis of stilbenoids I, biosynthesis of phenanthrenes, biosynthesis of flavone aglycones, and flavone and flavonol biosynthesis, all showed positive differential abundance scores, indicating that these pathways tend to be enriched in wild *S. australis*. Notably, pathways related to phenanthrene compounds, which are common in orchids, showed the strongest enrichment in wild *S. australis*. Moreover, all these pathways are based on the phenylpropanoid metabolic pathway. To explore the transcriptional basis underlying these interspecific metabolic differences, we performed a comparative transcriptome analysis between wild *S. sinensis* and *S. australis*. However, the differentially expressed genes (DEGs) identified did not show significant enrichment in the key metabolic pathways that were found to be differentially active at the metabolite level, such as phenylpropanoid, flavonoid, and phenanthrene biosynthesis.

Metabolite differences between wild and cultivated *S. sinensis*

Spiranthes species are terrestrial orchids with thick fleshy roots, hence the name 'Dragon's Beard Orchid' (*Pan long sen*). We propagated a batch of *S. sinensis* seedlings from seeds on solid medium, hardened them briefly in a greenhouse, and then carried out routine maintenance with essential nutrients. Leaves of the cultivated *S. sinensis* were relatively short and small. One-year-old cultivated plants possessed fewer fleshy roots, whereas two-year-old cultivated plants exhibited an increased number of fleshy roots and,

https://doi.org/10.48130/mpb-0026-0018

Table 1. Top 20 flavonoid metabolites with the highest relative abundances in wild *S. sinensis* and wild *S. australis*, respectively.

Compound	Class	Formula	Molecular weight (Da)	Rank in *S. sinensis*	Rank in *S. australis*
Isoscutellarein 7-O-glucoside (Isoscutellarein 7-glucoside)	Flavone	C21H20O11	448.1006	1	1
Amoenin	Flavonol	C21H20O11	448.1006	2	2
Rhamnetin 5-glucoside	Flavonol	C22H22O12	478.1111	3	3
Hesperetin-5-O-glucoside	Flavone	C22H24O11	464.1319	4	8
Quercetin-3,7-Di-O-glucoside	Flavonol	C27H30O17	626.1483	5	5
Meratin	Flavonol	C27H30O17	626.1483	6	10
Hypolaetin 7-sophoroside	Flavone	C27H30O17	626.1483	7	6
6-Hydroxykaempferol 3-methyl ether 6-glucoside	Flavonol	C22H22O12	478.1111	8	7
Quercetin 3-sambubioside-3'-glucoside	Flavonol	C32H38O21	758.1906	9	9
Hesperetin-8-C-glucoside-3'-O-glucoside	Flavanone	C28H34O16	626.1847	10	14
1,3,7-trihydroxy-4-prenylxanthone	Other Flavonoid	C18H16O5	312.0998	11	15
Cyanidin 3-O-beta-D-sambubioside	Anthocyanidin	C26H29O15	581.1501	12	13
Cinchonain Ib	Flavanol	C24H20O9	452.1107	13	
6-Hydroxykaempferol 3-methyl ether 6-glucoside	Flavonol	C27H30O17	626.1483	14	
Delphinidin-O-glucoside-O-xyloside-O-glucoside	Anthocyanidin	C32H39O21	759.1984	15	
Eriodictyol 5-O-glucoside	Flavanone	C21H22O11	450.1162	16	
2-(3,4-dihydroxyphenyl)-6,7-dihydroxy-4H-chromen-4-one	Flavone	C15H10O6	286.0477	17	16
Cyanidin 3-O-(beta-D-xylosyl-[1→2])-beta-D-galactoside)	Anthocyanidin	C26H29O15	581.1501	18	
Luteolin 5-glucoside	Flavone	C21H20O11	448.1006	19	17
Cyanidin 3-O-glucoside	Anthocyanidins	C21H21O11	449.1078	20	20
Maesopsin 4-O-glucoside (Hovetrichoside C)	Aurone	C21H22O11	450.1162		4
Phaseollidin	Isoflavone	C20H20O4	324.1362		11
2-(4-hydroxyphenyl)-7-methoxy-6-(3-methylbut-2-enyl)chromen-4-one	Flavone	C21H20O4	336.1362		12
3-{[(2R,3S,4R,5S,6S)-6-({[(2S,3R,4S)-3,4-dihydroxy-4-(hydroxymethyl) oxolan-2-yl]oxy}methyl)-3,4,5-trihydroxyoxan-2-yl]oxy}-5,7-dihydroxy-2-(4-hydroxyphenyl)chromen-4-one	Flavonol	C26H28O15	580.1428		18
Evolvuside B	Flavone	C21H20O11	448.1006		19

Numbers in the last two columns denote the rank order of relative abundance for each compound.

compared with wild plants, showed higher total biomass and root-to-shoot ratio (Fig. 1d; Supplementary Fig. S8). Metabolomic comparison of *S. sinensis* under different cultivation modes revealed that the total number of metabolites in wild plants was 32 and 37 fewer than in one-year-old and two-year-old cultivated plants, respectively (Supplementary Fig. S2). The numbers of amino acid derivatives, alkaloids, lipids, and terpenoids in wild plants were lower than those in cultivated plants; however, the number of flavonoids in wild plants was higher than in one-year-old cultivated plants but lower than in two-year-old cultivated plants (Supplementary Fig. S9). Comparison of the common metabolites among the three samples showed that 2,036 metabolites were detected in all three, accounting for 89.8% (wild *S. sinensis*), 88.6% (one-year-old cultivated), and 88.4% (two-year-old cultivated) of the total, indicating that cultivation mode had a minor effect on the overall metabolite composition. Moreover, the number of shared metabolites between the two cultivated samples was greater than that between wild and cultivated samples (Supplementary Fig. S10), suggesting that plants grown under the same cultivation mode have more similar metabolomic profiles. Sample correlation analyses based on different metabolite categories (Supplementary Fig. S5) showed the lowest correlation coefficients for flavonoids, ranging from 0.63 to 0.71 (Supplementary Fig. S5d), while primary metabolite correlations were higher, ranging from 0.90 to 0.93 (Supplementary Fig. S5b). This indicates that cultivation mode significantly affects flavonoid compounds but has a relatively minor impact on primary metabolites essential for basic life maintenance.

The clustering heatmap reflected differences in enriched metabolites among *S. sinensis* plants under different cultivation modes; in the vertical direction, the two cultivated samples clustered together first, then with the wild sample (Fig. 3a). K-means clustering of all metabolites revealed that 392, 692, and 458 metabolites were enriched in wild, one-year-old cultivated, and two-year-old cultivated *S. sinensis*, respectively (Fig. 3b–d; Supplementary Table S5), with the one-year-old cultivated plants accumulating the highest number. Compared with the other two groups, wild plants enriched more flavonoids, phenolic acids, alkaloids, lipids, and terpenoids; one-year-old cultivated plants enriched more amino acid derivatives, flavonoids, lipids, alkaloids, and terpenoids; two-year-old cultivated plants enriched more flavonoids, amino acid derivatives, alkaloids, phenolic acids, and terpenoids (Fig. 3e). Compared with wild plants, cultivated plants accumulated more primary metabolites, especially amino acid derivatives, while secondary metabolites such as flavonoids and alkaloids were enriched in all three groups, with the highest enrichment in two-year-old cultivated plants (Fig. 3e). Using K-means analysis specifically comparing wild and cultivated *S. sinensis*, overall cultivated plants accumulated more metabolites (Supplementary Fig. S11; Supplementary Table S6); amino acid derivatives, flavonoids, and alkaloids were more enriched in cultivated plants, with 98 more amino acid derivatives enriched in cultivated plants than in wild plants (Supplementary Fig. S12).

To further compare metabolite differences between wild and cultivated *S. sinensis*, we used VIP > 1, fold change > 2, and p-value < 0.05 to screen for metabolites significantly enriched in cultivated plants relative to wild plants (Supplementary Tables S7 and S8). The volcano plots (Fig. 4a, b) showed that, compared with wild plants, one-year-old and two-year-old cultivated plants enriched 480 and 428 metabolites, respectively, with more in the one-year-old group; these were mainly amino acid derivatives, flavonoids, terpenoids, alkaloids, and lipids (Fig. 4c). Between the two cultivated groups, 235 metabolites were commonly enriched, while 245 and 193 were specifically enriched in one-year-old and two-year-old plants,

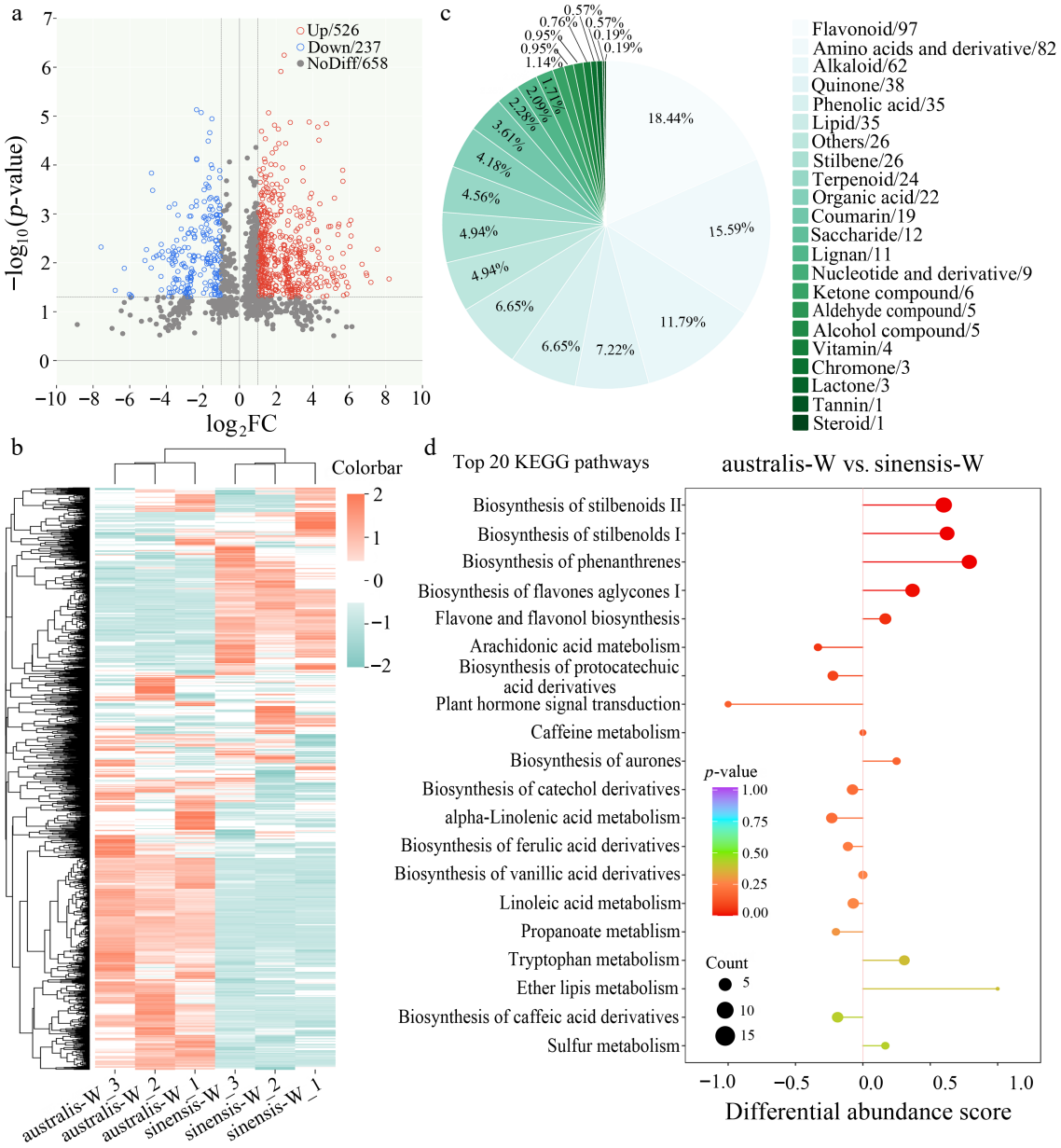

Fig. 2 Metabolites enriched in *S. australis*. (a) Differentially enriched metabolites in *S. australis* compared with *S. sinensis*. (b) Clustered heatmap analysis of metabolites from the two *Spiranthes* species. (c) Various categories of enriched metabolites in *S. australis* compared with *S. sinensis*. (d) KEGG enrichment analysis of differentially enriched metabolites in *S. australis* compared with *S. sinensis*.

respectively (Fig. 4d). KEGG pathway analysis of these enriched metabolites, based on the top 20 most significantly enriched pathways and their differential abundance scores (Fig. 4e, f), indicated that cultivated plants exhibited stronger metabolic synthesis activity than wild plants, particularly in the flavone and flavonol biosynthesis, flavonoid biosynthesis, biosynthesis of phenanthrenes, and biosynthesis of protocatechuic acid derivatives pathways.

Comparative transcriptomic analysis revealed significant changes in transcripts under different cultivation modes, with a large number of genes showing altered expression. Differentially expressed genes (DEGs) were systematically identified to generate high-throughput expression profiles. Compared with wild *S. sinensis*, one-year-old cultivated plants had 11,335 and 9,204 significantly up- and down-regulated genes, respectively (Fig. 5a). The significantly enriched biological processes included biosynthesis of secondary metabolites, flavonoid biosynthesis, starch and sucrose metabolism, and biosynthesis of amino acids (Fig. 5b). Among the top 20 KEGG pathways, 19 were metabolism-related, and most pathways contained more up-regulated than down-regulated genes (Supplementary Table S9). For two-year-old cultivated plants, 10,243 and 13,209 genes were significantly up- and down-regulated, respectively (Fig. 5c); KEGG analysis indicated these differentially expressed genes were mainly involved in diterpenoid biosynthesis, biosynthesis of various plant secondary metabolites, flavonoid biosynthesis, linoleic acid metabolism, and biosynthesis of secondary metabolites (Fig. 5d). Among the top 20 pathways, 17 were metabolism-related, with most showing more up-regulated than down-regulated genes (Supplementary Table S10). These transcriptomic results suggest that both one- and two-year-old cultivated *S. sinensis* have higher metabolite biosynthetic activity than wild plants.

https://doi.org/10.48130/mpb-0026-0018

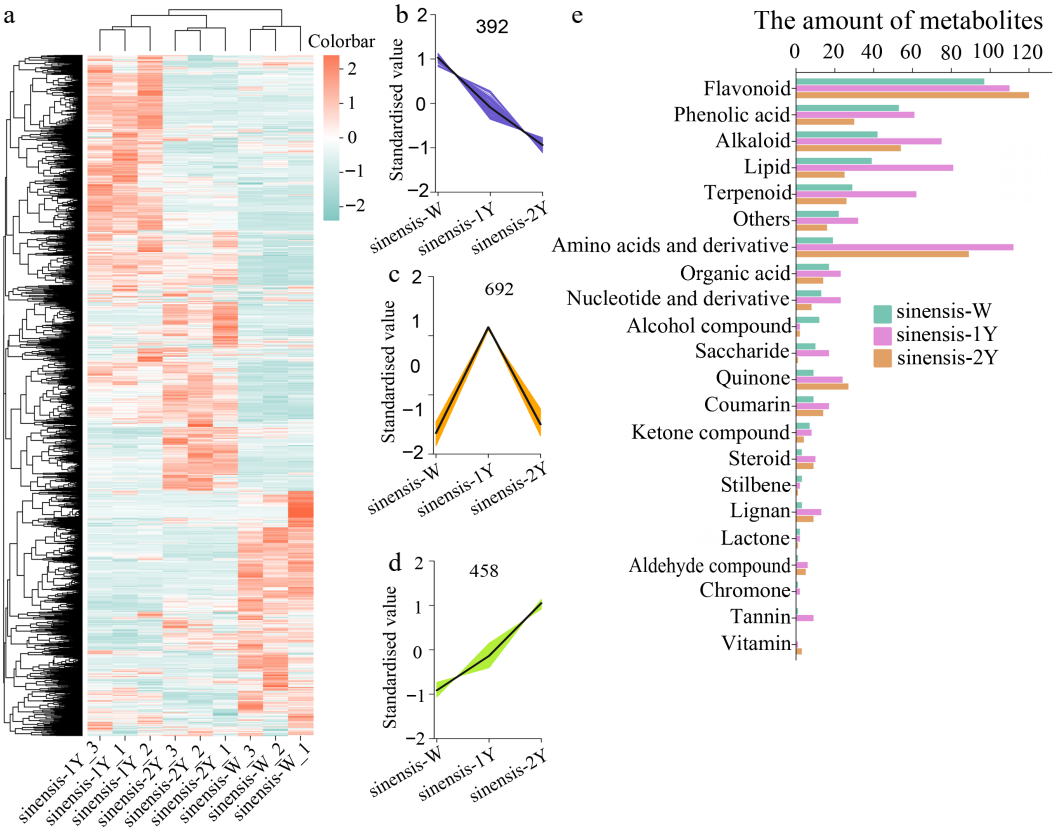

Fig. 3 Comparative metabolite profiling of *S. sinensis* under different cultivation modes. (a) Clustering heatmap analysis based on all metabolites. (b)–(d) K-means clustering analysis based on metabolite content. (e) Enrichment status of various classes of metabolites under different cultivation modes.

Metabolite differences between cultivated *S. sinensis* of different growth years

S. sinensis is a perennial herb that remains evergreen under suitable climatic conditions. Leaf buds emerge from the stem to produce leaves and inflorescences, and fleshy roots develop from the base of the stem. In the greenhouse, our cultivated plants grow year-round; due to ample nutrition, two-year-old plants produce multiple leaf buds from the short stem, resulting in greater biomass than one-year-old plants (Fig. 1d). Metabolomic comparison of one- and two-year-old cultivated plants (Supplementary Table S11) showed that the volcano plot (Fig. 6a) displayed enriched metabolites in both groups. One-year-old plants enriched more metabolites relative to two-year-old plants, mainly lipids (40), terpenoids (36), flavonoids (36), phenolic acids (31), and alkaloids (24), whereas two-year-old plants enriched more flavonoids (69 compounds), far exceeding other metabolite classes (Fig. 6b). KEGG pathway analysis of the differentially enriched metabolites (Fig. 6a) revealed that most of the top 20 pathways had negative differential abundance scores (Fig. 6c), indicating that the identified metabolites in these pathways tended to decrease, i.e., more metabolites were enriched in one-year-old cultivated plants. However, the anthocyanin biosynthesis, biosynthesis of flavone aglycones, and flavone and flavonol biosynthesis pathways showed positive scores, suggesting that anthocyanins, flavone glycoside derivatives, flavones, and flavonols tended to be enriched in two-year-old plants.

Transcriptomic analysis further compared gene expression between one- and two-year-old cultivated plants. Using fold change > 2 and p-value < 0.05 as thresholds, we identified 3,172 significantly up-regulated and 9,101 down-regulated genes in two-year-old compared with one-year-old plants, indicating that one-year-old plants had more up-regulated genes (Fig. 7b). KEGG analysis showed that these differentially expressed genes were most involved in metabolic pathways and biosynthesis of secondary metabolites (Fig. 7c). Among the top 20 KEGG pathways, 19 were related to metabolism, and most pathways had more down-regulated than up-regulated genes (Fig. 7c; Supplementary Table S12). Focusing on two flavonoid-related pathways, flavonoid biosynthesis and flavone and flavonol biosynthesis, we found that two-year-old cultivated plants had 35 highly expressed genes, significantly more than the nine highly expressed genes in one-year-old plants (Supplementary Fig. S13), which is consistent with the metabolomic result that two-year-old plants enriched more flavonoid compounds.

Discussion

In this context, our study presents a comprehensive comparative metabolomic analysis of two representative species, *S. sinensis* and *S. australis*, together with an assessment of how different cultivation strategies modulate secondary metabolite accumulation in *S. sinensis*. The metabolomic profiles of the two species were qualitatively similar but quantitatively distinct, with secondary metabolites—particularly flavonoids, alkaloids, and phenylpropanoid-derived compounds—showing the most pronounced interspecific differences, while primary metabolites remained largely stable. These findings align with previous comparative metabolomic studies indicating that closely related congeneric plant species typically exhibit pronounced differences in the abundance of secondary metabolites[27,28]. The minimal variation in primary metabolites between the two congeners aligns with the high genomic synteny

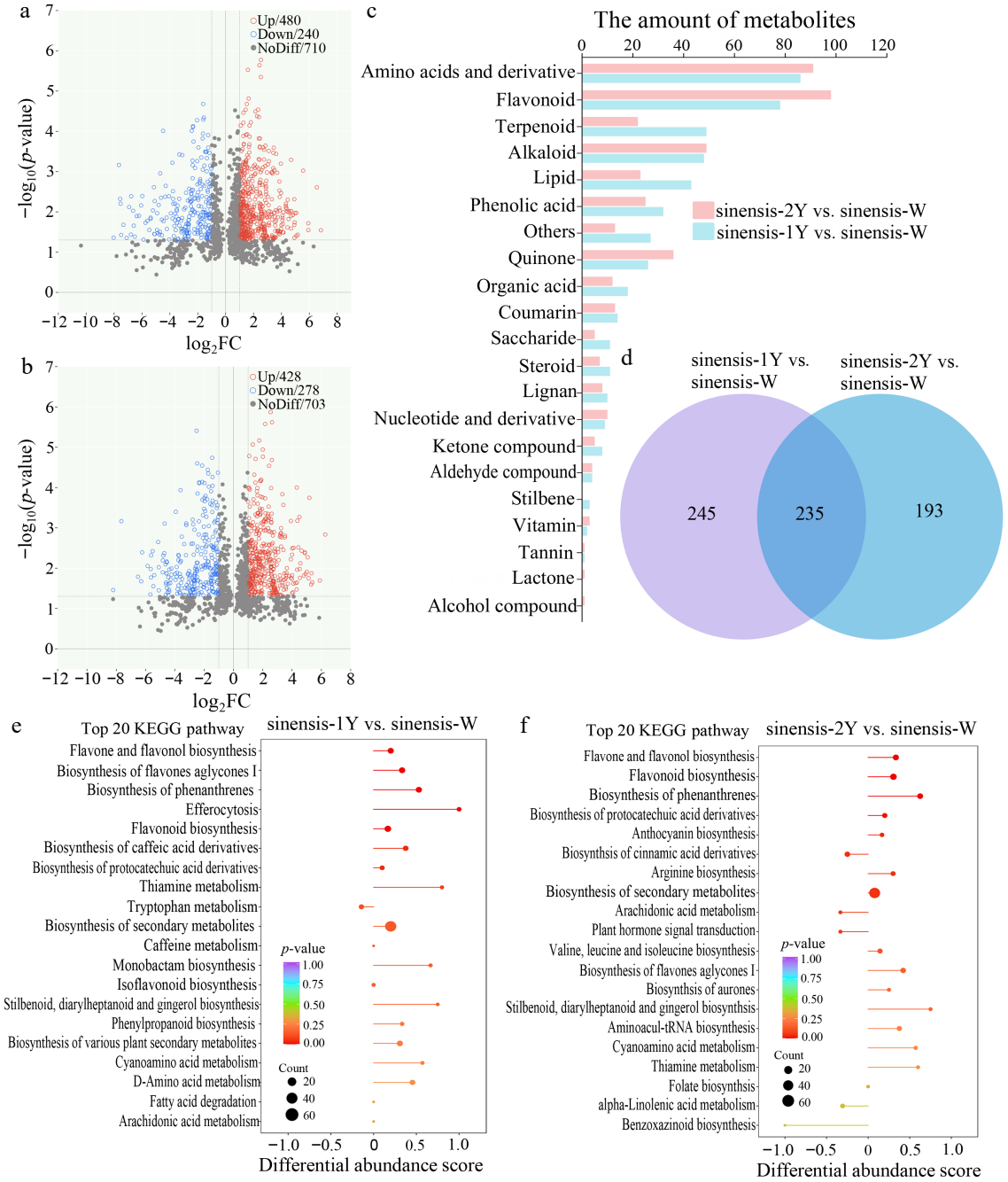

Fig. 4 Comparison of enriched metabolites in *S. sinensis* under different cultivation modes. (a) Differentially enriched metabolites between one-year-old cultivated *S. sinensis* and wild *S. sinensis*. (b) Differentially enriched metabolites between two-year-old cultivated and wild *S. sinensis*. (c) Different categories of metabolites enriched in cultivated *S. sinensis* compared with wild *S. sinensis*. (d) Venn diagram of metabolites enriched in cultivated *S. sinensis* compared with wild *S. sinensis*. (e) KEGG enrichment analysis of differentially enriched metabolites in one-year-old cultivated *S. sinensis*. (f) KEGG enrichment analysis of differentially enriched metabolites in two-year-old cultivated *S. sinensis*.

typically observed in closely related species, where core housekeeping functions are under strong stabilizing selection. In contrast, the biosynthesis and accumulation of secondary metabolites are more susceptible to environmental influences and display greater phenotypic plasticity[29], thereby contributing to the observed interspecific divergence in secondary metabolism.

Given the pharmacologically active metabolites isolated from '*Pan long sen*' previously[4–6], wild *S. australis* demonstrates significantly greater enrichment of bioactive constituents than *S. sinensis*, particularly phenanthraquinones, stilbenes, and flavonoids. *S. australis* exhibits a quantitatively more abundant and diverse secondary metabolome, particularly in phenylpropanoid-derived compounds, suggesting distinct phytochemical profiles that may underlie differential ethnopharmacological applications. Collectively, these results indicate heightened activity of the phenylpropanoid metabolic network in wild *S. australis*, which likely underpins the enhanced biosynthesis and accumulation of a broader array of structurally and functionally diverse bioactive metabolites. However, unlike well-characterized medicinal plants such as *Panax ginseng* or *Artemisia annua*, no single bioactive compound has yet been established as a

https://doi.org/10.48130/mpb-0026-0018

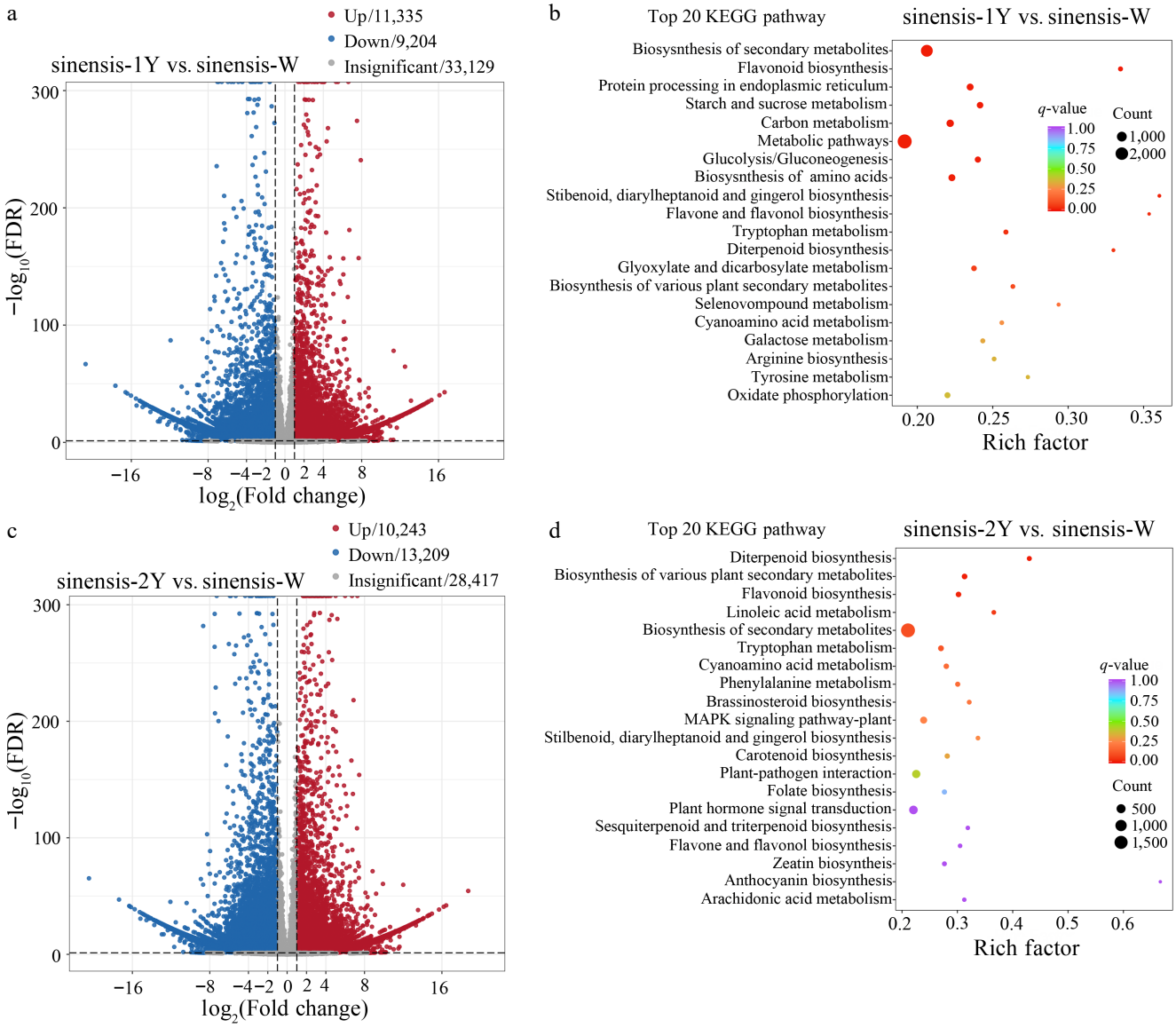

Fig. 5 Comparative transcriptomic analysis of *S. sinensis* under different habitats. (a) Volcano plot of DEGs between one-year-old cultivated and wild *S. sinensis*. (b) KEGG enrichment profiles of DEGs between one-year-old cultivated and wild *S. sinensis*. (c) Volcano plot of DEGs between two-year-old cultivated and wild *S. sinensis*. (d) KEGG enrichment profiles of DEGs between two-year-old cultivated and wild *S. sinensis*.

definitive chemical marker for any *Spiranthes* species[5]. As a result, current methodologies based on quantification of individual active ingredients are insufficient for reliably assessing or comparing the medicinal quality among *Spiranthes* congeners. Therefore, the unambiguous identification and pharmacological validation of signature bioactive constituents in *S. sinensis*, *S. australis*, and other closely related taxa should be established as a priority in future phytochemical and pharmacological research[6]. Such endeavors will not only enable precise botanical authentication of '*Pan long sen*' but also lay the scientific foundation for the targeted breeding and selection of elite germplasm with optimized phytochemical profiles for pharmaceutical applications.

A striking observation was the disconnect between transcriptomic and metabolomic profiles in the interspecific comparison between *S. sinensis* and *S. australis*: despite pronounced metabolic differences, the corresponding DEGs showed no significant enrichment in the phenylpropanoid or flavonoid pathways. This transcriptome–metabolome uncoupling is not unusual in plant systems[30] and can be attributed to multiple, non-mutually exclusive mechanisms. Beyond the previously considered post-transcriptional regulation, temporal asynchrony, and genome assembly limitations, we note that transcriptional regulators—such as MYB, bHLH, and WRKY transcription factors—play central roles in modulating phenylpropanoid flux, often independently of the transcript abundance of structural genes. Although the lack of a reference genome prevented us from confidently assigning specific transcriptional factors (TFs) to target pathways, we identified a large number of unigenes with homology to these families among the DEGs (Supplementary Table S13), and their differential expression patterns between *S. sinensis* and *S. australis* suggest potential regulatory roles. Moreover, metabolic feedback inhibition—where pathway end products suppress their own synthesis—and the spatial separation of biosynthesis (leaf) and storage (tuberous root) may further obscure gene–metabolite correlations in whole-plant extracts. Future studies employing tissue-specific transcriptomics and targeted TF functional assays will be essential to resolve these regulatory hierarchies.

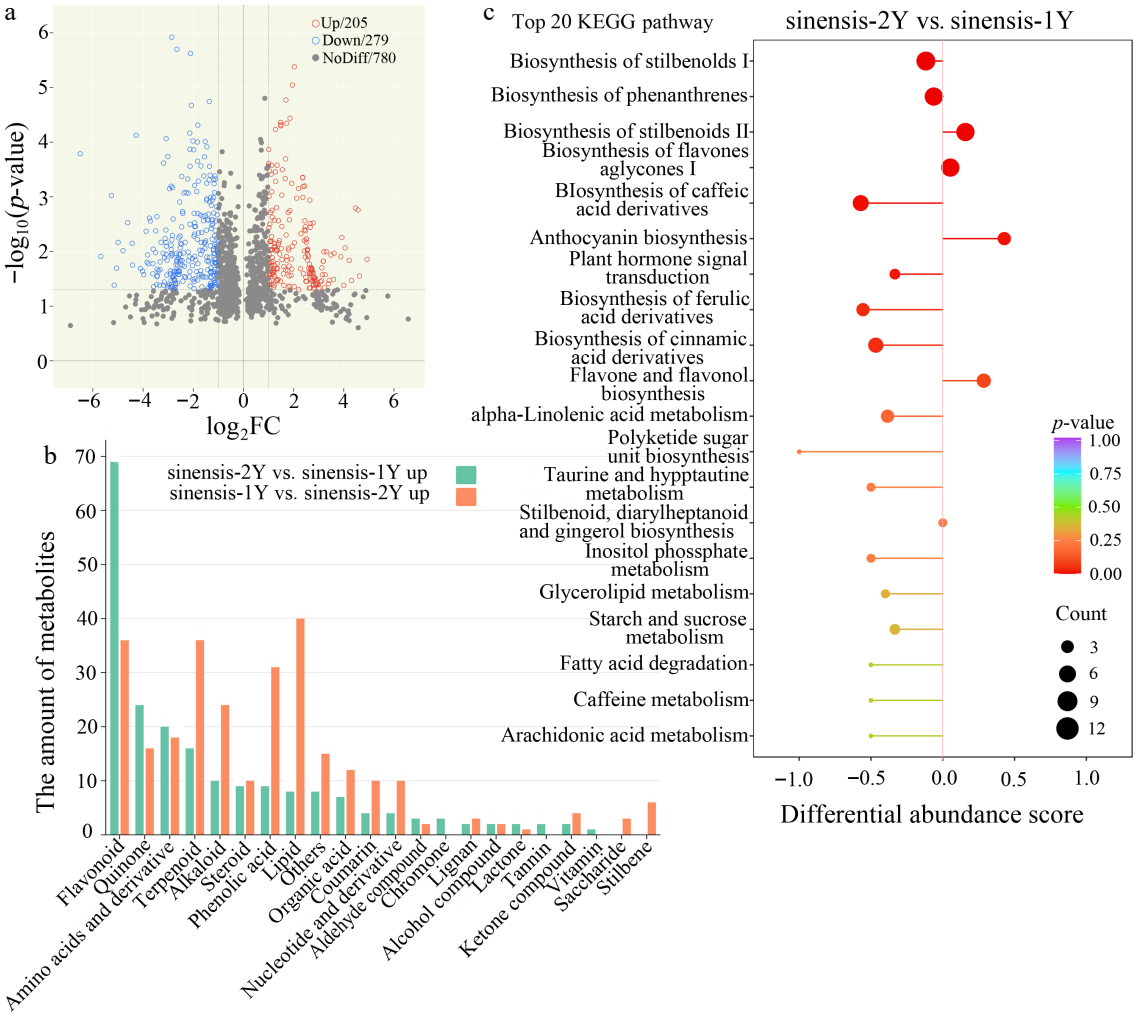

Fig. 6 Comparison of metabolites in cultivated *S. sinensis* of different ages. (a) Differentially enriched metabolites in cultivated *S. sinensis* of different ages. (b) Different categories of the enriched metabolites. (c) KEGG enrichment analysis of differentially enriched metabolites in two-year-old cultivated *S. sinensis*.

Beyond inherent genetic differences, our research on cultivated *S. sinensis* demonstrates that environmental and agronomic factors serve as potent modulators of its medicinal quality. The transition from wild to cultivated conditions induced profound metabolic reprogramming in *S. sinensis*, with cultivated plants accumulating broader classes of secondary metabolites, especially amino acid derivatives, flavonoids, alkaloids, and terpenoids. This enhancement is likely multifactorial. Optimized macronutrient (N, P, K) and water supply under greenhouse conditions[31,32] certainly alleviate resource constraints, providing the primary metabolic substrates necessary for secondary pathway activity, as supported by the coordinated upregulation of structural genes in phenylpropanoid and flavonoid biosynthesis (Fig. 5b, d). Furthermore, other environmental factors probably contribute as well. Wild *S. sinensis* grows under forest canopies where light quantity and quality (low red/far-red ratio) often suppress flavonoid biosynthesis via cryptochrome and phytochrome signaling; greenhouse cultivation, by contrast, provides uniform high-light conditions that may promote photoprotective flavonoid accumulation. Rhizosphere microbial communities also differ substantially between native forest soils and artificial substrates; recent evidence indicates that cultivation can reshape the rhizosphere microbiome, which in turn modulates secondary metabolism through microbial-derived signaling molecules[33]. Additionally, wild plants experience a suite of biotic and abiotic stresses (herbivory, pathogens, drought) that, while potentially inducing certain defensive metabolites, also drain carbon and nitrogen reserves from primary metabolism. The relatively stress-free greenhouse environment, combined with ample nutrition, may thus liberate resources for sustained secondary pathway flux. We cannot quantify the relative contributions of these factors, but we propose that they collectively underpin the enhanced metabolic capacity observed in cultivated *S. sinensis*.

Our comparative metabolomic and transcriptomic analyses revealed a distinct developmental shift in metabolic programming between one- and two-year-old *S. sinensis*. One-year-old plants exhibited broader metabolic diversity and higher expression of genes associated with general biosynthetic pathways, consistent with active vegetative growth. In contrast, two-year-old plants underwent a marked transition toward specialized metabolism, characterized by enhanced accumulation of high-value flavonoids and concerted upregulation of structural genes in their biosynthetic pathways. This temporal reprogramming suggests a classic 'growth-maturation trade-off' in perennial medicinal herbs: during the first year, metabolic resources are primarily allocated to rapid biomass accumulation and primary protection, whereas, in the second year,

https://doi.org/10.48130/mpb-0026-0018

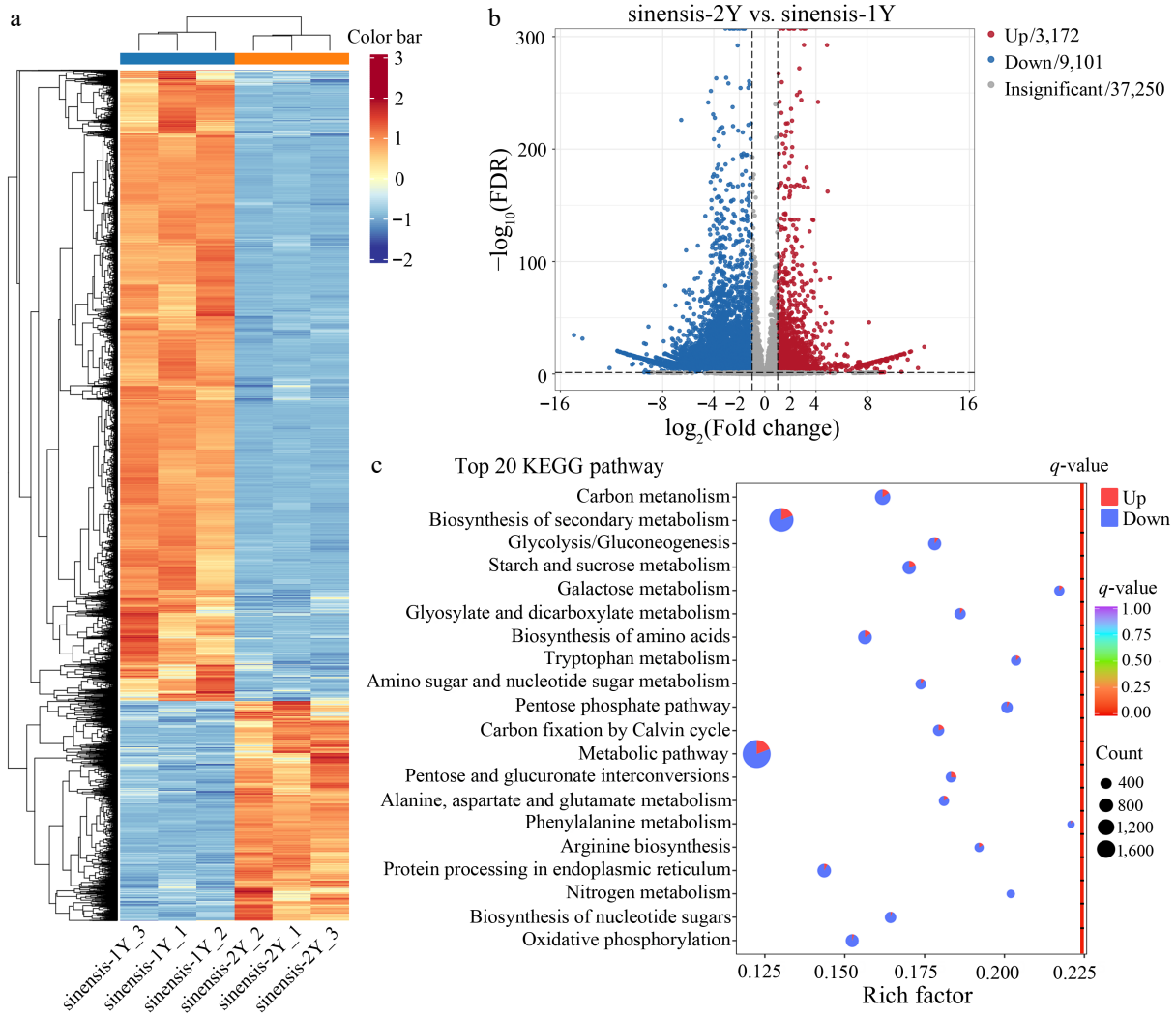

Fig. 7 Comparative transcriptomic analysis of cultivated *S. sinensis* across different growth years. (a) Heatmap of DEGs among different cultivation years. (b) Volcano plot of DEGs between two-year-old and one-year-old cultivated *S. sinensis*. (c) KEGG enrichment analysis of DEGs between two-year-old and one-year-old cultivated *S. sinensis*.

flux is progressively redirected toward the biosynthesis of flavonoid glycosides, possibly as a long-term storage strategy in fleshy tuberous roots—a pattern analogous to that observed in other perennial rhizomes like *Cibotium barometz*[24]. Nevertheless, these intrinsic age-dependent dynamics must be interpreted within the context of agronomic management. For perennial medicinal species, prolonged cultivation often coincides with sustained fertilizer application, which can substantially alter the rhizosphere microenvironment by inducing shifts in microbial community composition, nutrient imbalances, pH fluctuations, and reduced aeration[31]. Such changes in the soil microbiome, in turn, modulate nutrient availability and can either stimulate or suppress secondary metabolism via microbial-derived signaling molecules[33]. Although the present study did not include rhizosphere microbiome data, the observed decline in certain non-flavonoid secondary metabolites in two-year-old plants raises the possibility that this 'trade-off' may be further compounded by nutrient competition or altered substrate availability over extended cultivation. This hypothesis warrants dedicated future investigation integrating metagenomic and ionomic approaches to decouple the intrinsic developmental program from extrinsic soil-derived factors.

A notable limitation of this study is the use of whole-plant samples for metabolomic profiling. Given that fleshy roots might be the primary medicinal organs in '*Pan long sen*', our whole-plant data may dilute organ-specific accumulation patterns. Future work employing spatial metabolomics or organ-specific transcriptomics will be essential to precisely map the tissue localization of key bioactive flavonoids and phenanthrenes. Despite this caveat, our comparative analysis unequivocally demonstrates that genetic identity (species) and agronomic practices (cultivation duration and conditions) are orthogonal determinants of medicinal quality in the two studied *Spiranthes* species.

Conclusions

Our findings provide a comprehensive metabolomic and transcriptomic basis for understanding species-specific metabolic signatures between *S. australis* and *S. sinensis*. We demonstrate that *S. australis* possesses a quantitatively more abundant and diverse secondary metabolome than *S. sinensis*, highlighting its potential as a high-value chemotype for pharmaceutical applications.

Furthermore, we establish that artificial cultivation, particularly extended growth duration, serves as a critical agronomic strategy for maximizing flavonoid yield in *S. sinensis*. These results provide a robust scientific rationale for the selective breeding of *S. australis* and for optimizing cultivation protocols to enhance the production of flavonoid-rich biomass. Future studies encompassing a wider range of *Spiranthes* taxa will be required to determine whether the metabolic features observed here are conserved across the genus, and spatial metabolomics or organ-specific transcriptomics will be essential to precisely map the tissue localization of key bioactive compounds.

Author contributions

The authors confirm their contributions to the paper as follows: study conception and design: Wang FP, Yan YH; preparation of plant materials: Zhou SR; data collection, analysis and interpretation of results, manuscript revision: Wang FP, Zhao PP; draft manuscript preparation: Wang FP, Chen LJ, Zhao PP. All authors reviewed the results and approved the final version of the manuscript.

Data availability

All data generated or analyzed during this study are included in this published article and its supplementary information files. The raw reads were uploaded to the NCBI BioProject database under Accession No. PRJNA1497119. The company delivers a processed quantitative results table containing the characteristic ion peak areas (i.e., relative abundance values) for all detected metabolites across all samples for widely targeted metabolomics assays (Supplementary Table S14). This processed table serves as the primary data matrix for all downstream analyses.

Acknowledgments

This study was supported by the Science and Technology Program of the Shenzhen Key Basic Research Project (Grant No. JCYJ20220818103212025) and the Central Financial Transfer Payment Project of the National Forestry and Grassland Administration (Monitoring of Nationally Protected Plants: *Vanilla shenzhenica* and *Alsophila costularis*).

Conflict of interest

The authors declare that they have no conflict of interest.

Supplementary information accompanies this paper online at: https://doi.org/10.48130/mpb-0026-0018.

Dates

Received 21 July 2026; Revised 10 September 2026; Accepted 17 September 2026; Published online 23 September 2026

References

[1] Hussein RA, El-Anssary AA. 2019. Plants secondary metabolites: the key drivers of the pharmacological actions of medicinal plants. In *Herbal Medicine*, ed. Builders PF. London: IntechOpen. pp. 11–30 doi: 10.5772/intechopen.76139

[2] Latif R, Nawaz T. 2026. Medicinal plants and human health: a comprehensive review of bioactive compounds, therapeutic effects, and applications. *Phytochemistry Reviews* 25:2299–2342

[3] Lin YL, Huang RL, Don MJ, Kuo YH. 2000. Dihydrophenanthrenes from *Spiranthes sinensis*. *Journal of Natural Products* 63:1608–1610

[4] Liu J, Li CY, Zhong YJ, Yang L, Li YF. 2013. Chemical constituents from *Spiranthes sinensis*. *Biochemical Systematics and Ecology* 47:108–110

[5] Yan Y, Wu C, Zhou H, Feng X, Li YF. 2019. Secondary metabolites from *Spiranthes sinensis* (Orchidaceae). *Biochemical Systematics and Ecology* 86:103910

[6] Kuo YJ, Pei JK, Chao WW. 2022. Pharmacological and chemical potential of *Spiranthes sinensis* (Orchidaceae): a narrative review. *Plants* 11:1692

[7] Li CY, Liu J, Su XH, Yuan ZP, Zhong YJ, et al. 2013. New dimeric phenanthrene and flavone from *Spiranthes sinensis*. *Journal of Asian Natural Products Research* 15:417–421

[8] Tezuka Y, Nagashima K, Hirano H, Kikuchi T. 1989. Spiranthesol, a dimeric dihydrophenanthrene from the roots of *Spiranthes sinensis* (Pers.) Ames var. *amoena* (M. Bieberson) Hara. *Chemical and Pharmaceutical Bulletin* 37:1667–1669

[9] Tezuka Y, Ji L, Hirano H, Ueda M, Nagashima K, et al. 1990. Studies on the constituents of orchidaceous plants. IX. Constituents of *Spiranthes sinensis* (Pers.) Ames var. *amoena* (M. Bieberson) Hara. (2). Structures of spiranthesol, spiranthoquinone, spiranthol-C, and spirasineol-B, new isopentenyldihydrophenanthrenes. *Chemical and Pharmaceutical Bulletin* 38:629–635

[10] Ji M, Wang Y, Wang Y, Zhang X, Liu C, et al. 2025. A new dihydrophenanthrene with cell viability enhancing activities from *Spiranthes sinensis*. *Records of Natural Products* 19:101–106

[11] Kovács A, Vasas A, Hohmann J. 2008. Natural phenanthrenes and their biological activity. *Phytochemistry* 69:1084–1110

[12] Shie PH, Yang CP, Huang GJ, Wang SY, Kuo YH. 2020. Sinensol-C isolated from *Spiranthes sinensis* inhibits adipogenesis in 3T3-L1 cells through the regulation of adipogenic transcription factors and AMPK activation. *Molecules* 25:4204

[13] Liang CP, Chang CH, Liang CC, Hung KY, Hsieh CW. 2014. *In vitro* antioxidant activities, free radical scavenging capacity, and tyrosinase inhibitory of flavonoid compounds and ferulic acid from *Spiranthes sinensis* (Pers.) Ames. *Molecules* 19:4681–4694

[14] Peng JY, Han X, Xu LN, Qi Y, Xu YW, et al. 2008. Two new prenylated coumarins from *Spiranthes sinensis* (Pers.) Ames. *Journal of Asian Natural Products Research* 10:279–283

[15] Zou M, Wang R, Yin Q, Liu L. 2021. Bioassay-guided isolation and identification of anti-Alzheimer's active compounds from *Spiranthes sinensis* (Pers.) Ames. *Medicinal Chemistry Research* 30:1849–1855

[16] Li Y, Zhao W, Zuo X, You J, Xing M, et al. 2025. Habitat changes due to cultivation alter the genetic diversity and secondary metabolic changes of medicinal plants. *Scientific Reports* 15:36185

[17] Turker H. 2025. Investigation of the physiological and antioxidant properties of the medicinal and endemic *Hypericum bilgehan-bilgilii* species under different cultivation methods. *Biology* 14:1302

[18] Hou C, Huang L, Li Z, Sun N, Yang S, et al. 2024. Domestication of medicinal plants (*Lonicera japonica* Thunb.) in China: comparison of morphological, resistance and biochemical traits between wild and cultivated populations. *Frontiers in Plant Science* 15:1501396

[19] Hao Y, Zhang Z, Luo E, Yang J, Wang S. 2025. Plant metabolomics: applications and challenges in the era of multi-omics big data. *aBIOTECH* 6:116–132

[20] Pace MC, Giraldo G, Frericks J, Lehnebach CA, Cameron KM. 2019. Illuminating the systematics of the *Spiranthes sinensis* species complex (Orchidaceae): ecological speciation with little morphological differentiation. *Botanical Journal of the Linnean Society* 189:36–62

[21] Yu G, Wang LG, Han Y, He QY. 2012. clusterProfiler: an R package for comparing biological themes among gene clusters. *OMICS: A Journal of Integrative Biology* 16:284–287

[22] The Gene Ontology Consortium, Aleksander SA, Balhoff J, Carbon S, Cherry JM, et al. 2023. The gene ontology knowledgebase in 2023. *Genetics* 224:iyad031

[23] Kanehisa M, Furumichi M, Sato Y, Kawashima M, Ishiguro-Watanabe M. 2023. KEGG for taxonomy-based analysis of pathways and genomes. *Nucleic Acids Research* 51:D587−D592

[24] Wang FP, Chen LJ, Zhou SR, Tang M, Zhang X, et al. 2025. Integrated metabolomic and transcriptomic analyses reveal temporal dynamics of secondary metabolite accumulation in *Cibotium barometz* rhizome. *Frontiers in Plant Science* 16:1702726

[25] Padhee S, Kerry RG, Champati BB, Mohanty D, Mohanty S, et al. 2026. Medicinal orchids as anti-inflammatory agents: phytochemistry and molecular mechanisms of action. *South African Journal of Botany* 192:294−335

[26] Tóth B, Hohmann J, Vasas A. 2018. Phenanthrenes: a promising group of plant secondary metabolites. *Journal of Natural Products* 81:661−678

[27] Wu X, Yuan Y, Yang Y, Yan M, Yang Q, et al. 2026. Comparative metabolomics and transcriptomics analysis of *Rosa roxburghii* tratt and *Rosa kweichonensis* var. sterilis. *Molecules* 31:831

[28] Liu L, Li Q, Alami M, Shen R, Zhu J, et al. 2026. Comparison of metabolite differences and pharmacologically active constituents between *Piper longum* and *Piper sarmentosum* based on non-targeted metabolomics. *PeerJ* 14:e20719

[29] Bacler-Żbikowska B, Hutniczak A, Pilawa B, Chodurek E, Zdybel M, et al. 2025. The current state of knowledge about changes in the synthesis of the secondary metabolites caused by habitat conditions and microbial activity. *Agronomy* 15:2251

[30] Fernie AR, Stitt M. 2012. On the discordance of metabolomics with proteomics and transcriptomics: coping with increasing complexity in logic, chemistry, and network interactions scientific correspondence. *Plant Physiology* 158:1139−1145

[31] Bernstein N, Gorelick J, Zerahia R, Koch S. 2019. Impact of N, P, K, and humic acid supplementation on the chemical profile of medical cannabis (*Cannabis sativa* L). *Frontiers in Plant Science* 10:736

[32] Simonutti M, Berhongaray G, Derita M, Zabala JM. 2025. Response of *Cannabis sativa* L. to inorganic fertilization (N, P, K): biomass, nutrient uptake and cannabinoids profile. *International Journal of Plant Biology* 16:92

[33] Song F, Fu D, Wang A, Yang Z, Yu T. 2026. Effects of different cultivation methods on the rhizosphere microbial community and secondary metabolites of *Houttuynia cordata* Thunb. *PeerJ* 14:e20797